

To be presented at the First World  
Congress of Nuclear Medicine, Tokyo,  
Japan, September 30-October 4, 1974.

LBL-3000

RECEIVED  
LAWRENCE  
RADIATION LABORATORY

III 19 1974

LIBRARY AND  
DOCUMENTS SECTION

LIQUID XENON MULTIWIRE PROPORTIONAL  
CHAMBERS FOR NUCLEAR MEDICINE APPLICATIONS

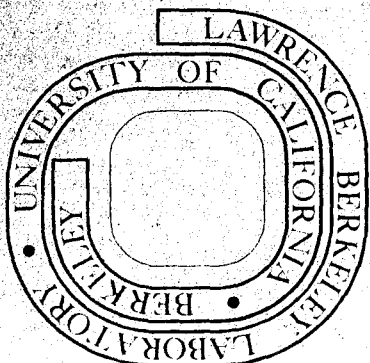
H. Zaklad, S. E. Derenzo,  
T. F. Budinger and L. W. Alvarez

May 1974

Prepared for the U. S. Atomic Energy Commission  
under Contract W-7405-ENG-48

**For Reference**

Not to be taken from this room



LBL-3000  
21

LIQUID XENON MULTIWIRE PROPORTIONAL CHAMBERS FOR NUCLEAR MEDICINE APPLICATIONS. H. Zaklad, S. E. Derenzo, T. F. Budinger, and L. W. Alvarez, Lawrence Berkeley Laboratory, University of California, Berkeley, California, U. S. A.

The need for improved spatial resolution in nuclear medicine has long been recognized. Notable attempts to achieve this goal are the gas-filled wire chambers and solid-state detectors.<sup>(1)</sup> However, at energies above 100 keV, gas-filled chambers suffer from poor detection efficiency and a long recoil electron range in the gas. While it is advantageous to pressurize these chambers to 10 or more atmospheres, structural design of the thin window presents a formidable task. High-resolution optimal collimators do not appear to have sufficient strength to be used as a pressure support window. Solid-state detectors, while having the potential of a gamma camera with a superb energy resolution, are presently studied on a very small scale due to technological and cost limitations.

Aside from the detector, the parallel-hole collimator presents a real limit to the resolution of the camera. A factor of two improvement in the resolution results in a factor of four loss in the collimator's transmission. A careful analysis of optimal collimators and the application of collimators designed for a specific depth range and resolution are part of our overall program.

Our goal has been the development of a liquid-xenon multiwire gamma camera with 2- to 3-mm spatial resolution, high counting-rate performance, high sensitivity, and the potential for scaling-up in size. Important ingredients for successful imaging in the prototype chamber discussed in this paper were the discovery of electron multiplication in liquid xenon,<sup>(2)</sup> the development of reliable purification techniques,<sup>(3)</sup> and the ability to extract electrons from the liquid into the gaseous phase.

This paper is specifically addressed to the subject of detector development with liquid-xenon totally-filled chambers and recent work with dual-phase chambers in which the  $\gamma$  rays are converted in the liquid phase and are electronically detected in the gaseous phase.

Electron Multiplication in a Single-Wire Chamber: Detailed measurements of the electron avalanche process in liquid xenon were made in a single-wire 8-mm-diam. chamber, using anode diameters of 2.9, 3.5, and 5.0  $\mu$ .<sup>4</sup> The photopeak pulse height (typically 25% FWHM) due to the 279-keV gamma rays was measured as a function of the applied voltage. At a field of  $E = 2 \times 10^6$  V/cm, the first Townsend coefficient is  $\alpha = (4.5 \pm 0.3) \times 10^4$ /cm. Pulse-height saturation occurs at a gain of  $\approx 200$  regardless of wire diameter, and a drop in the pulse height is observed when the chamber is radiated with more than 200 counts/sec per millimeter of length: both suggest space-charge limitations. It was possible to reliably reproduce the single-wire chamber runs at any time and electrical discharges were not a problem. In general, we found that electron avalanche occurs in liquid xenon at an electric field  $27 \pm 3$  times smaller than would be predicted using measurements made in gaseous xenon, and  $E/\rho$  density scaling (where  $\rho$  is the density).

Other workers have learned to produce crystals of xenon in a single-wire chamber that were perfect enough for counting,<sup>(5)</sup> and had gain characteristics similar to what we observe in the liquid.

Liquid-Xenon Filled Multiwire Camera: The basic properties of the liquid-xenon camera and preliminary images were previously reported.<sup>(6-8)</sup> The chamber is 1.5-cm thick with arrays of 24 anode wires, spaced 2.8 mm apart, and 24 cathode strips with the same spacing. For a totally filled mode of operation, the anode wire diam. is 3.5- $\mu$

tungsten. In order to maintain the same avalanche amplification in a multiwire chamber as in a single-wire chamber having the same wire diameter, the voltage at the cathode must be scaled up by a factor of 2.2. Typically, we operate at 5 kV and an avalanche gain of  $\approx 30$ . The energy resolution when the liquid is properly cleaned is  $\approx 25\%$  FWHM ( $^{203}\text{Hg}$ -279 keV). In this chamber a concentration of 50 ppb of oxygen corresponds to a 5% contribution to the energy resolution. The liquified gas from our purification system<sup>(3)</sup> is further cleaned by reversing the cathode potential to cause electron emission from the anode wires. Occasionally at high gains internal discharges take place that appear as background dots on the display oscilloscope. (This observation motivated us to explore the operation of a dual-phase mode as described in a later section.)

Figure 1 shows the  $^{203}\text{Hg}$ -279 keV images of the letters XE. Slots corresponding to the shape of the letters were cut in a slab of lead 2.5 cm thick. The slots were machined in a focused orientation so that a point source 12 cm under the slab could project the letters on a plane above the slab. This approach produces an image over an extended area, using a point source. The left image in Fig. 1 was taken using the amplifier-per-line readout to be described in a later section. The letters were tilted with respect to the anode-cathode coordinates of the camera. Two of the anode lines were inoperative and the resulting black strips indicate the camera's limit of resolution. Application of the amplifier-per-line readout resulted in an improved image quality over images obtained earlier using the charge division readout.<sup>(8)</sup> On the right in Fig. 1 is the image of the same source, as taken by the scintillation camera.

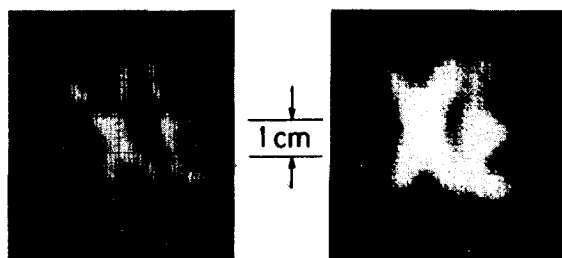


Fig. 1. Comparison of images of letters cut in a lead block. Source is  $^{203}\text{Hg}$ -279 keV. Right image was taken by the scintillation camera; left image was taken by the 6 cm $\times$ 6 cm liquid xenon camera. The latter was tilted with respect to the X, Y coordinates. Two of the anode lines were inoperative and the resulting black strips indicate the camera's limit of resolution.

A rat was injected intravenously with 100  $\mu\text{Ci}$  of  $^{99\text{m}}\text{Tc}$ -sulfur colloid. The collimator used here was designed to maximize the transmission while maintaining the minimal septa leakage path of 3 attenuation lengths,<sup>(9)</sup> and was made of corrugated lead sheets of 0.15-mm septa spaced between flat sheets to generate a triangular hole of 0.85mm height. The hole length is 12 mm. The transmission in air is  $\approx 10^4$  counts/sec per mCi.

The image of the rat's liver shown in Fig. 2 contains 10,000 dots. The inactive line crossing the image horizontally is due to a damaged field-effect transistor (FET). When the rat was moved away, the background of the camera was 25 dots/sec. For the rat's

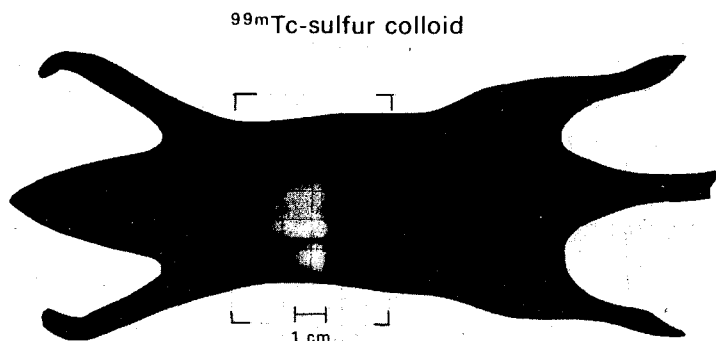


Fig. 2. Image of rat's liver using 100  $\mu\text{Ci}$  of  $^{99\text{m}}\text{Tc}$  sulfur colloid superimposed on a schematic outline of the animal. An inactive anode line crosses the image horizontally. The image was taken using a lead collimator of a resolution  $\approx 3$  mm FWHM.

liver, the calculated image resolution is  $\approx 4$  mm FWHM.

**Dual-Phase Camera:** The prospect of having high gain in the gas, while retaining the advantages of liquid xenon as a conversion medium, motivated us to operate the camera in a dual-phase mode.<sup>(10)</sup> We have learned the following:

a. In a simple ionization chamber partially filled with 2 mm of liquid xenon and at a given voltage, the pulse height due to either  $\alpha$  or  $\gamma$  sources diminished with time. By momentarily grounding the high voltage, the pulse height was restored. It is postulated that the electronegative impurities attach to the free electrons, migrate in the liquid to the gas-liquid interface and stay there. The space charge formed reduces the electric field in the liquid and inhibits the incoming electrons from passing through the interface. The pulse height was stabilized by providing an additional grounded electrode in the liquid that would neutralize the charged electronegative impurities.

b. A Frisch gridded ionization chamber and an  $\alpha$  source ( $^{241}\text{Am}$ ) were used to measure the fraction of electrons actually reaching the anode as a function of the electric field in the liquid (Fig. 3). Xenon was allowed to condense to a height of 1 mm. The data were corrected for recombination, electron capture, and grid transmission. Electric fields were calculated assuming a dielectric constant of 1.88 for liquid xenon. (Note that above 2 kV/cm, 90% of the electrons are extracted.) The preliminary data indicates that the extraction efficiency for electrons is a rather steep function of the electric field. When the liquid is not very pure and the electron attachment coefficient  $\sigma$  exceeds 0.1/mm drift, higher fields are required to extract the electrons and the curve shifts to the right.

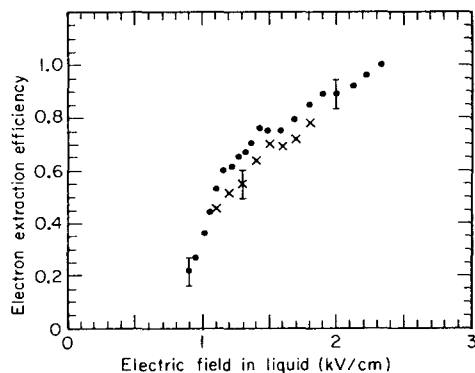


Fig. 3. Electron extraction efficiency from liquid xenon region into the gaseous xenon region in the dual-phase, Frisch gridded ionization chamber as a function of the electric field in the liquid.

In the dual-phase mode the FWHM of the  $\alpha$  pulses does not seem to be affected much by the extraction process. At a field of 2.7 kV/cm the pulse height distribution of the  $\alpha$ 's has so far been measured as FWHM = 23%. When the chamber was totally filled with liquid xenon, a FWHM as high as 25% has been observed. (Effects of amplifier noise were not considered.)

c. The 24-wire, 6 cm  $\times$  6 cm camera was operated in a dual-phase mode using 13- $\mu$ -diam. anode wires and a liquid level 1.4 mm (Fig. 4). In order to enhance the field at the gas-liquid interface above the lower cathode, while limiting the field on the wires, the upper cathode was maintained at the anode potential. At 4200 volts a point source of  $^{57}\text{Co}$  (122 keV) was imaged at four positions under the

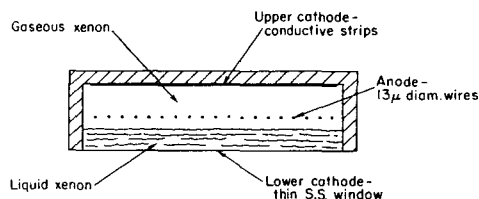


Fig. 4. A schematic of a liquid-xenon gamma camera operating in a dual-phase mode. The gamma ray is converted in the liquid. Ionization electrons are extracted from the liquid into the gas region and multiply on the 13- $\mu$ -diam. anode wires.

camera as shown on Fig. 5. The gain in the gas was  $> 100$ . Note that the inherent resolution of the camera of  $\approx 3$  mm FWHM is preserved. The sensitivity variation among these points is  $\approx 7\%$  (which can easily be explained by liquid level variations). The liquid-gas dual-phase camera is limited to imaging in the horizontal plane only. When other orientations of multiple views (such as in three-dimensional imaging) are desired a solid-gas dual-phase detector could serve as an alternate approach. The problem of growth of a large xenon crystal operating as a detector has not yet been solved.

Readout: An earlier readout scheme<sup>(6,7)</sup> consisted of two charge-sensitive amplifiers connected to an array of capacitors coupled between the chamber wires. Position was determined by dividing the charge appearing at one end of the capacitor array by the sum of the charge. We found that this method suffered from a poor signal-to-noise ratio when operating with the totally filled chamber due to the high capacitive loading at the amplifier input.

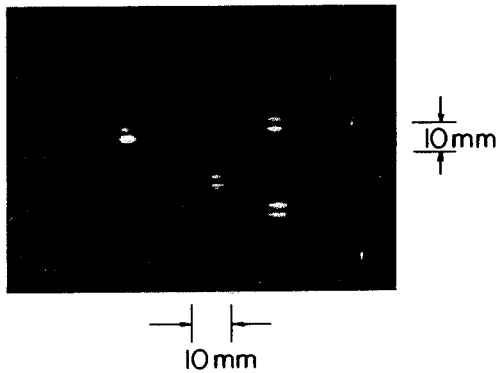


Fig. 5. Four images of a point source taken by the liquid-xenon gamma camera operating in a dual-phase mode. The source,  $^{57}\text{Co}$ -122 keV, was  $\approx 2$  mm diam. at the chamber. The source was repositioned after each image was taken. Count uniformity was within  $\pm 3.5\%$  from one source position to the other. Horizontal and vertical coordinates have different scales.

The new approach employs one charge-sensitive amplifier-per-line followed by a window discriminator (Fig. 6). The pulses originating at the anode are integrated at  $2 \mu\text{sec}$  and differentiated at  $5 \mu\text{sec}$  in order to maximize the signal-to-noise ratio. The charge-sensitive amplifier rms noise is  $1 \times 10^{-16} \text{C}$ . The pulses pass between low- and high-level comparators at the anode and the position is digitized. If more than one anode triggers, the data are rejected. At the cathode the pulses must exceed a lower-level comparator before digitizing. A digital circuit computes the center of gravity of the induced charge and the data are checked for coincidence between the anode and the cathode. The beam intensifier Z and the X, Y information (via two digital-to-analog converters) are transferred to the oscilloscope. The dead-time currently is set for  $\approx 3 \mu\text{sec}$  but can be reduced to  $\approx 1 \mu\text{sec}$  for direct communication to a computer.

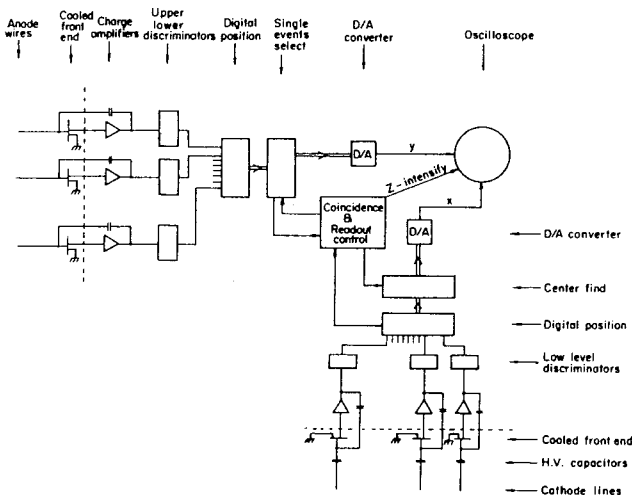


Fig. 6. An amplifier-per-line readout schematic. The charge is amplified and selected by the discriminator window. At the anode, the digital information is rejected when more than one anode is triggered. At the cathode, the center of gravity of the induced charge is digitally calculated. After anode-cathode coincidence is checked, the digital data is converted into analog voltages. The scope beam is turned on (Z intensify) to display the X, Y information.

The advantages of the amplifier-per-line are:

1. High signal-to-noise ratio. (limited by front FET noise)
2. Pulse-height selection per line allows for an improved spatial resolution by rejecting multiple interactions in the detector.
3. When more than a single event is detected, the data are rejected to eliminate the anode-cathode coincidence ambiguity.
4. Since each line acts independently, the counting rate is limited by the anode cathode coincidence rate rather than by the pulse rise and fall time.
5. Inter wire gain variations can be compensated by amplifier gain adjustments.

The disadvantages are:

1. The charge on the cathode is distributed over several strips, hence, smaller pulses are induced on each.
2. Cost is relatively high.

Induced Charge on the Cathode: The charge induced on the cathode in gas-filled chambers is known to be due to the motion of the positive ions after avalanche near the anode. As a result, the induced charge is spread over a large area to cathodes located many millimeters away. This spread was measured in a 24-wire chamber operating in a totally filled mode (Fig. 7). The pulse height was recorded at a cathode strip as a point source ( $< 2$  mm FWHM) was moved in increments of 2.5 mm. We have observed that both upper and lower cathodes receive equal amounts of charge due to the avalanche. The strip under the center of gravity of the induced charge receives only  $\approx 10\%$  of the total induced charge. Digital circuits interpret the data coming from several strips and locate the center of the induced charge within  $\pm \frac{1}{2}$  strip (twice the resolution of the anode). The relatively small charge appearing on the center cathode strips ( $\approx 3 \times 10^{-15}$  C at 140 keV) requires a low-noise charge amplifier. The present readout is operating at  $0.1 \times 10^{-15}$  C rms noise. In a dual-phase operation, on the other hand, the gain is higher ( $> 100$ ), which may allow for an implementation of a simplified readout scheme as a much larger amount of charge is available at the cathode.

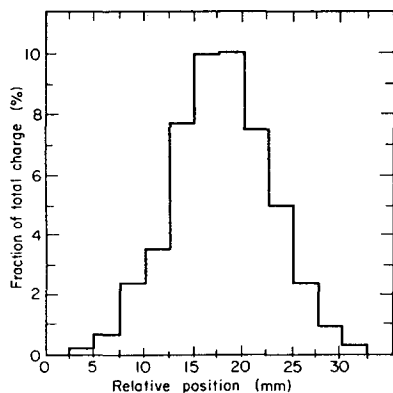


Fig. 7. The charge induced on the cathode in a totally liquid-filled chamber. The pulse height was recorded at a cathode strip as a point source ( $< 2$  mm FWHM at the chamber) was moved in increments of 2.5 mm.

Wire Irregularities: In liquid xenon the distance required for the avalanche to grow by a factor of  $e$  (inverse of the first Townsend coefficient) is about  $0.2 \mu$  at  $2 \times 10^6$  V/cm. Thus, the gain is very sensitive to variations in wire diameter. In reality, this is not a serious problem since we found that selected wires may exhibit only 2 to 3% pulse height variation along the chamber length. Other wires exhibiting large gain variations along their length can be preferentially replaced. The presence of dust particles on the wires in the chamber was a source of gain nonuniformity, hot spots and spurious discharges. The particles may be introduced either from the purifier, from the vacuum gauges (hot or cold filaments), or by improper cleaning of the chambers. The problem was solved by more careful handling of the chamber and by the addition of a  $0.1 \mu$  millipore filter at the inlet of the chamber. In a dual-phase mode at 4200 V as described above, the inverse of the first Townsend coefficient is  $2 \mu$ . Thus we expect the gain in gas to be one-tenth as sensitive to wire variations as the gain in liquid.

Conclusions: Images produced by the liquid-xenon camera demonstrate a spatial resolution governed by the wire spacing of  $\approx 3$  mm. The dual-phase camera retains the same resolution as a totally filled chamber while the avalanche gain available in the gas is substantially higher. The inability of the dual-phase camera to image on non-horizontal planes, because of the liquid level requirements, may be overcome by freezing the liquid into a working crystal.

Proper collimator design and utilization, in conjunction with a high resolution camera, could provide nuclear medicine with the means for significantly improved clinical procedures.

#### Acknowledgments

We gratefully acknowledge the contributions of Alan Kirschbaum, Richard Muller, Robbie Smits, Terry Mast, Takehiro Tomitani, and Pete Schwemin. We are indebted to Joe Savignano and Tony Vuletich for the construction and care of our systems. We also thank Bill Jackson and Tom Shimizo for designing and debugging the electronic readout. Work was supported in part by the NIH and in part by the U. S. Atomic Energy Commission.

#### References

1. Papers on these subjects may be found in IEEE Trans. Nucl. Sci., NS-20(1) and NS-21(1).
2. R. A. Muller, S. E. Derenzo, G. Smadja, D. B. Smith, R. G. Smits, H. Zaklad, and L. W. Alvarez, Phys. Rev. Lett. 27, 532 (1971).
3. Haim Zaklad (D. Eng. Thesis), Lawrence Radiation Laboratory Report UCRL-20690 (1971).
4. S. E. Derenzo, T. S. Mast, H. Zaklad, and R. A. Muller, Lawrence Berkeley Laboratory Report LBL-1313, March (1973), to be published, Phys Rev. A, June 1974
5. A. F. Pisarev, V. F. Pisarev, G. S. Revenko, Sov. Phys. —JETP 36, 828 (1973).
6. H. Zaklad, S. E. Derenzo, R. A. Muller, G. Smadja, R. G. Smits, and L. W. Alvarez, IEEE Trans. Nucl. Sci., NS-19(3) 206 (1972).
7. H. Zaklad, S. E. Derenzo, R. A. Muller, and R. G. Smits, IEEE Trans. Nucl. Sci. NS-20(1) 429 (1973).
8. S. E. Derenzo, T. F. Budinger, R. G. Smits, H. Zaklad, and L. W. Alvarez, Lawrence Berkeley Laboratory Report LBL-2092, May 1973.
9. Hal O. Anger, Inst. Soc. Am. Trans. 5, 311 (1966).
10. B. A. Dolgoshein, V. N. Lebedenko, and B. V. Rodionov, JETP Lett., 11, (11) 351 (1970). These authors operated a dual-phase chamber using liquid argon, and measured electron extraction from the liquid into the gas.